

# A physical interpretation of the variability power spectral components in accreting neutron stars

Adam Ingram<sup>1\*</sup> & Chris Done<sup>1</sup>

<sup>1</sup>*Department of Physics, University of Durham, South Road, Durham DH1 3LE, UK*

Submitted to MNRAS

## ABSTRACT

We propose a physical framework for interpreting the characteristic frequencies seen in the broad band power spectra from black hole and neutron star binaries. We use the truncated disc/hot inner flow geometry, and assume that the hot flow is generically turbulent. Each radius in the hot flow produces fluctuations, and we further assume that these are damped on the viscous frequency. Integrating over radii gives broad band continuum noise power between low and high frequency breaks which are set by the viscous timescale at the outer and inner edge of the hot flow, respectively. Lense-Thirring (vertical) precession of the entire hot flow superimposes the low frequency QPO on this continuum power.

We test this model on the power spectra seen in the neutron star systems (atolls) as these have the key advantage that the (upper) kHz QPO most likely independently tracks the truncation radius. These show that this model can give a consistent solution, with the truncation radius decreasing from  $20 - 8 R_g$  while the inner radius of the flow remains approximately constant at  $\sim 4.5 R_g$  i.e. 9.2 km. We use this very constrained geometry to *predict* the low frequency QPO from Lense-Thirring precession of the entire hot flow from  $r_o$  to  $r_i$ . The simplest assumption of a constant surface density in the hot flow matches the observed QPO frequency to within 25 per cent. This match can be made even better by considering that the surface density should become increasingly centrally concentrated as the flow collapses into an optically thick boundary layer during the spectral transition. The success of the model opens up the way to use the broad band power spectra as a diagnostic of accretion flows in strong gravity.

**Key words:** X-rays: binaries – accretion, accretion discs

## 1 INTRODUCTION

Black holes and neutron stars have very similar gravitational potentials as neutron star radii are approximately the size of the last stable orbit. Thus their accretion flows should be similar despite the fundamental difference in the nature of the central object: neutron stars have a solid surface, while black holes do not. This similarity is seen in the spectral and timing properties. Both black hole binaries (BHB) and disc accreting neutron stars (atolls) show a distinct transition between hard spectra seen at low luminosities (termed the low/hard state in BHB and the island state in atolls) and much softer spectra seen at high luminosities (high/soft in BHB, banana branch in atolls). During the transition, the properties of the rapid variability also change. This variability can be approximately described as band limited continuum noise between a low and high frequency break, with a low frequency Quasi-Periodic Oscillation (hereafter LF QPO) superimposed. The low frequency break and LF QPO move to higher frequencies as the source spectrum softens

in both BHB and atolls whereas the high frequency break is seen to remain approximately constant. Atoll power spectra also display a pair of kHz QPOs, a feature not (unambiguously) observed in BHB power spectra. The peak frequency of these QPOs is seen to increase as the source spectrum softens such that it correlates with the break frequency and the LF QPO. (see e.g. the reviews by van der Klis 2005, hereafter vdK05; McClintock & Remillard 2006, hereafter MR06; and Done, Gierlinski & Kubota 2007, hereafter DGK07)

Both spectral and variability behaviour can be qualitatively explained if the geometrically thin, cool accretion disc is replaced at radius  $r_o$  by a hot inner flow which produces the hard Comptonised spectrum. As this transition radius decreases, the disc spectrum increases in luminosity and temperature and more soft seed photons from the disc illuminate the corona. This increases the Compton cooling so the hard spectrum softens slightly. This effect becomes much stronger when the disc extends far enough down in radii to overlap with the hot flow, and the Comptonised spectrum softens dramatically with decreasing radius as the disc approaches the last stable orbit. Throughout this evolution, all the timescales for vari-

\* E-mail: a.r.ingram@durham.ac.uk

ability associated with the inner edge of the thin disc decrease. This broadly explains the correlated spectral-timing behaviour observed in both BHB and atolls if the low frequency break and LF QPO are set by  $r_o$  (Barret 2001; DGK07).

There have been some quantitative tests of the spectral evolution predicted by these models as the components which make up the energy spectra (disc and comptonisation) are well understood (e.g. Chaty et al 2003; Done & Gierlinski 2003; Gierlinski, Done & Page 2008; Cabanac et al 2008). However, there is no comparable consensus on the fundamental components which make up the power spectra. This is especially evident in the case of the LF QPO. This is a clear characteristic frequency, most probably associated with  $r_o$ , yet it cannot be used to quantitatively determine  $r_o$  until its physical origin is well understood. While there are a plethora of potential mechanisms in the literature (e.g. Fragile et al 2001; vdK05; Titarchuk & Osherovich 1999; 2000), our recent model of Lense-Thirring (vertical) precession of the hot inner flow is the first to simultaneously explain both its spectral and timing properties (Ingram, Done & Fragile 2009, hereafter IDF09).

Lense-Thirring precession is a relativistic effect whereby a spinning black hole with its angular momentum misaligned with that of the binary system produces a torque. This propagates via bending waves throughout the hot flow, and can make the entire flow within  $r_o$  vertically precess as a solid body (though it does not *rotate* as a solid body: orbits are still approximately Keplerian). The precession frequency is set by the outer radius of the vertically precessing flow,  $r_o$ , the dimensionless black hole spin parameter,  $a_*$ , and the inner radius of the hot flow,  $r_i$ , for a given mass,  $M$ . The precession frequency of the flow increases as  $r_o$  decreases until  $r_o \rightarrow r_i$  when the thin disc extends underneath the hot flow at all radii, suppressing vertical modes. IDF09 showed that this model gives a good match to the observed LF QPO behaviour for BHB as a class for  $r_o$  decreasing  $50 \rightarrow r_i$  (where all radii are in units of  $R_g = GM/c^2$ ) assuming that  $r_i$  is set by the increased torque from the misaligned flow rather than by the last stable orbit (Fragile et al 2007, 2009, Fragile 2009).

Here we develop a full model for the power spectrum, encompassing the broad band noise as well as the LF QPO. The only previous attempt at such a combined model is Titarchuk & Osherovich (1999), though the physical mechanism for modulation of their LF QPO is not clear. However, the broad band noise components are beginning to be well understood. Numerical simulations now give some insight into the nature of the noise generating process. Angular momentum transport in the accretion flow takes place via stresses (a.k.a. ‘viscosity’) generated by the Magneto-Rotational Instability (MRI: Balbus & Hawley 1998). This process generates fluctuations in all quantities (e.g. Krolik & Hawley 2002). However, the mass accretion rate at any given radius cannot change faster than the local viscous timescale, so fluctuations at each radius are damped on this timescale (Lyubarskii 1997; Psaltis & Norman 2000; also see Titarchuk & Osherovich 1999; Misra & Zdziarski 2008 for a slightly different approach). Coupling this to the truncated disc/hot flow geometry gives a prediction of self-similar fluctuation power between timescales corresponding to the viscous timescale at the inner and outer radii of the hot flow (Churazov et al 2001; Arevelo & Uttley 2006). Thus the evolution of the continuum power spectrum can determine the inner and outer radii of the flow, and these can be used to *predict* the LF QPO frequency, to compare with that observed.

While we could do this in the BHB systems, the atolls give additional constraints as the spin of the neutron star is often independently known from burst oscillations (e.g. Strohmayer, Markwardt,

& Kuulkers 2008; Piro & Bildsten 2005). Neutron star power spectra also contain the upper and lower kHz QPOs (e.g. vdK05) together with an additional high frequency noise component (Sunyaev & Revnivtsev 2000). The upper kHz QPO (ukHz QPO) is most likely the Keplerian frequency at the truncation radius  $r_o$  (e.g. van der Klis et al 1996; Stella & Vietri 1998; Schnittman 2005) and the narrowness of the feature means that this gives an unambiguous determination of  $r_o$ . This identification independently constrains a key parameter of the LF QPO model. Hence here we use the atolls to outline a self-consistent model for *all* the observed components in the power spectrum.

## 2 THE ORIGIN OF THE BROAD BAND POWER SPECTRUM

We choose atoll sources with multiple observations showing the power spectral evolution so as to test the model over a wide range of  $r_o$ . We consider only low spin systems ( $a_* < 0.3$ ), because higher spins lead to an equatorial bulge of the neutron star which distorts space-time from being well described by the Kerr metric (Miller et al 1998). This leads us to pick the atoll systems 4U 1728-34 and 4U 0614+09 (van Straaten et al 2002), both of which have spin  $a_* \sim 0.2$  and (assumed) mass  $M \sim 1.4M_\odot$ .

Typical power spectra of 4U 1728-34 and 4U 0614+09 are shown in the top and bottom panels respectively of Figure 1. We see that the QPOs described above are superimposed on a complex, broad band noise continuum. This can be approximately modelled by a twice broken power law, following  $P(\nu) \propto \nu^0$  below the lower break frequency  $\nu_b$ ,  $P(\nu) \propto \nu^{-2}$  above the higher break frequency  $\nu_h$  and  $P(\nu) \propto \nu^{-1}$  between (i.e a flat top in  $\nu P(\nu)$ ). However, multiple Lorentzians give a much better description of the broad band noise (Belloni, Psaltis & van der Klis 2002; Fig 1). Each of these has a characteristic frequency,  $\nu_c$ , and width,  $\Delta\nu$ , which can be combined together into a quality factor  $Q = \nu_c/\Delta\nu$ . The lowest frequency component,  $L_b$ , is generally a zero centred Lorentzian, so it peaks in  $\nu P(\nu)$  at  $\Delta\nu$ , producing the low frequency ‘break’ in the flat top noise. This break frequency correlates with the LF QPO and kHz QPOs (Wijnands & van der Klis 1999; Klein-Wolt & van der Klis 2008; Psaltis, Belloni & van der Klis 1999) whereas the high frequency ‘break’ (sometimes referred to as the hectohertz QPO) varies much less (e.g. vdK05; DGK07).

### 2.1 Outer radius

This behaviour of the high and low frequency breaks can be qualitatively explained in the truncated disc/hot inner flow model. The inner radius of the flow remains constant at the neutron star radius, so giving the constant high frequency power, while the outer radius sweeps inwards, leading to the progressive loss of low frequency components (Gierlinski, Nikolajuk & Czerny 2008). Quantitatively this can be modelled by each radius generating noise power as a zero centred Lorentzian with width  $\Delta\nu = \nu_{visc}$ . The viscous frequency  $\nu_{visc} = 1.5\alpha(h/r)^2\nu_\phi$ , where  $\alpha$  is the Shakura-Sunyaev viscosity parameter,  $h/r$  is the disc semi-thickness and  $\nu_\phi$  is the rotational frequency of fluid particles within the flow. However, none of these are necessarily straightforward to define. MRI simulations of black hole accretion flows show that  $\alpha$  and  $h/r$  vary with radius (e.g. Fragile et al 2007, 2009). Additionally,  $h/r$  should change during state transitions as the hot inner flow collapses. In neutron stars especially, this collapse marks the transition from the hard X-ray emission region being an extended optically thin boundary

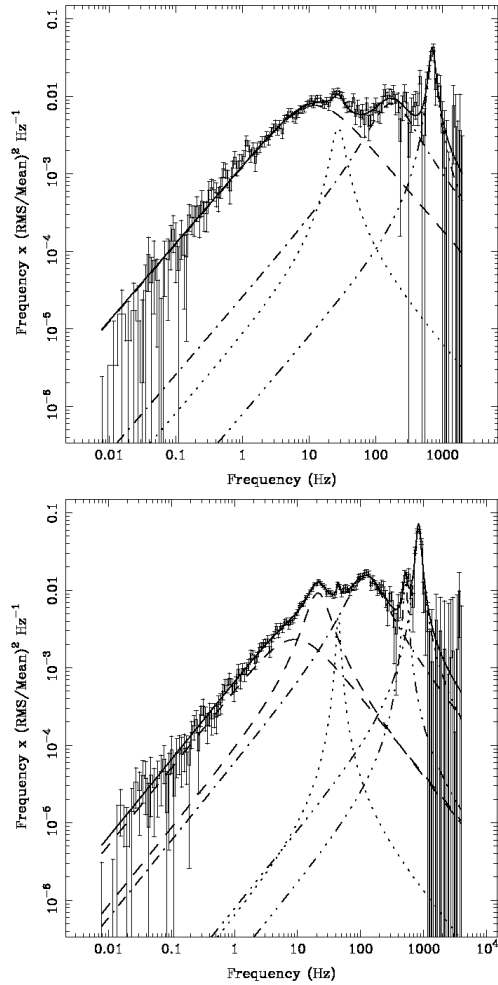


**Figure 1.** Power spectra and fit functions for 4U 1728-34 (top) and 4U 0614+09 (bottom), reproduced with the permission of van Straaten et al (2002) and the AAS. Lorentzians represent the following components: the lower break  $L_b$  (dashed), the LF QPO (dotted), the high frequency break  $L_h$  (dot-dashed) and the kHz QPOs (triple dot-dashed). When there are two dashed lines present, as in the bottom panel, we will refer to the left hand one as  $L_{b2}$  and the right hand one as  $L_{VLF}$  with one assumed to be a continuation of  $L_b$ .

layer which merges smoothly onto the hot inner flow, to a much more compact boundary layer. As well as the impact of such a transition on  $h/r$ , the viscosity mechanism in the boundary layer may well be very different to that of the standard MRI, and the azimuthal velocity field is dominated by that of the star rather than being Keplerian.

This makes neutron stars somewhat more complex than black holes. However, their saving grace is that we can use their additional kHz QPOs to independently determine  $r_o$  assuming that  $\nu_{ukHz} = \nu_k(r_o) = c/[2\pi R_g(r_o^{3/2} + a_*)]$  (it should be safe to assume  $\nu_\phi$  at the inner edge of the *disc* to be Keplerian). The blue triangular points in Figure 2 show that this requires  $r_o$  to decrease from  $20 - 8R_g$ , consistent with the expected change in radius from the spectral softening seen from the island state to the lower banana branch (Barret 2001).

The square magenta points in Figure 2 show the high frequency break (hertz) frequency, which remains approximately constant as discussed earlier and the crossed orange points show the

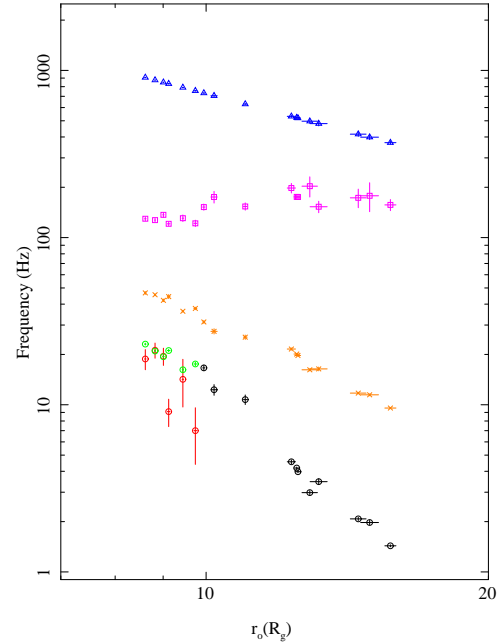


**Figure 2.** Plot of characteristic frequencies plotted against  $r_o$  as inferred from the assumption  $\nu_{ukHz} = \nu_k(r_o)$ . The blue triangular points represent  $\nu_{ukHz}$  and the square magenta points represent  $\nu_h$ . The orange crossed points represent the LF QPO frequencies and the circular points the low frequency break. The black points are for power spectra where there is no ambiguity over what the break frequency is whereas the red points are for  $\nu_b = \nu_{b2}$  and the green points for  $\nu_b = \nu_{VLF}$ .

LF QPO frequency. This correlates with the low frequency break (e.g. Wijnands & van der Klis 1999), which is represented by the circular points. Of these, the black points represent data where  $\nu_b$  is unambiguously identified in the power spectra. However, this becomes difficult at the highest kHz QPO frequencies (i.e. smallest radii) as there is an additional component observed in the low frequency power spectrum e.g. the lower panel of Figure 1, where two low frequency Lorentzians are required. It is not immediately clear which one of these corresponds to  $\nu_b$  e.g. van Straaten et al (2002) refer to the lowest frequency Lorentzian as  $L_b$  and call the other  $L_{VLF}$  while Altamirano et al (2008) put  $L_b$  on the right and term the other  $L_{b2}$ . Here we only use  $L_b$  where this break is unambiguously determined by the data. Where there are two competing low frequency components we refer to the lowest frequency one as  $L_{b2}$  and the other as  $L_{VLF}$ . The green points in Figure 2 represent  $\nu_{VLF}$  whereas the red points represent  $\nu_{b2}$ . The green points connect smoothly onto the black points where  $\nu_b$  is unambiguously determined, while the red points do not. Thus it seems most likely that the higher of the two low frequency components represents the continuation of the break frequency determined by  $r_o$ .

Of these 6 points with a split break frequency, 4 are from observations of 4U 1728-34 and 2 from 4U 0614+09. If we analyse the colour-colour diagram of 4U 1728-34 (Di Salvo et al 2000), we see that these 4 observations (9-12 of 19) occur just before the transition between the island state and the banana branch. Intriguingly, the geometry inferred from models of the spectral evolution require an *overlap* between the hot flow and truncated disc close to the transition. The splitting of the break frequency then has an obvious interpretation with the outer radius of the hot flow being larger than the inner radius of the thin disc. The hot flow in this overlap region will have smaller scale fluctuations, as the size scale

of the magnetic field is limited by the thin disc in the mid plane. Thus  $\nu_{b2}$  can be interpreted as the viscous frequency at the edge of the corona with  $\nu_{VLF}$  being the viscous frequency at the truncation radius.

## 2.2 Inner radius

We assume that the lower break frequency,  $\nu_b$  is identified with  $\nu_{visc}(r_o)$ , and we use the independent constraints on  $r_o$  from the kHz QPO above to track out the unknown variation in  $\nu_{visc}$  ( $\propto \alpha(h/r)^2 \nu_\phi(r)$ ). We parameterise this as a power law, so that  $\nu_b = \nu_{visc}(r_o) = Ar_o^{-\gamma}$ . We then use the best fit values of  $A$  and  $\gamma$  derived from the low frequency break to determine  $r_i = [(A\nu_h)]^{1/\gamma}$  assuming that the high frequency break in the noise power (hertz component) is the viscous frequency at  $r_i$ .

However, as discussed in the previous section, we do not necessarily expect this power law representation of  $\nu_{visc}(r)$  to stay constant as the truncation radius sweeps in and the source spectrum softens due to the collapse of the more extended hot flow into the boundary layer, with its potentially very different viscosity and azimuthal velocity. Instead we split the radial range in  $r_o$  into four groups of points, each described by a different best fit power law. The top panel of Figure 3 shows this best fit power law relation for each group of points, with a clear change in both slope and normalisation as the truncation radius moves inwards. Quantitatively, the inferred value of  $\gamma$  moves from 3.25 (blue), 3.02 (magenta), 2.88 (green) to 2.69 (red). We can now use our moving power law representation in order to extrapolate values for  $r_i = [(A\nu_h)]^{1/\gamma}$  taking care to use the correct values of  $\gamma$  and  $A$  for a given value of  $\nu_h$ .

The lower plot of Fig. 3 shows the derived values for  $r_i$  with error bars including the systematic error in determining the best fit values of  $A$  and  $\gamma$ . We infer from this that the radius of the neutron star lies at  $r_i \approx 4.5 \pm 0.04 \approx 9.2 \pm 0.1$  km. This would mean that the neutron star is slightly smaller than its own last stable orbit ( $5.3 R_g$  for  $a_* = 0.2$ ), indicating a soft equation of state, but we caution that the exact value depends on the accuracy of our assumed power law representation of the viscous frequency with radius. Any more complex form will extrapolate to a different inner radius, and the value of this radius may also be affected by time dilation. Nonetheless, the remarkable constancy of the derived inner radius gives some confidence in our approach, and the value of 9.2 km is very close to the ‘canonical’ assumption of 10 km for a  $1.4M_\odot$  neutron star.

## 3 TESTING LENSE-THIRRING IN ATOLLS

Now we have both the inner and outer radius for the hot flow, we can directly calculate the predicted Lense-Thirring precession frequency. However, there is one additional free parameter which is the mass distribution in the hot flow, which can be parameterised by  $\zeta$ , the radial dependence of the surface density,  $\Sigma = \Sigma_i(r/r_i)^{-\zeta}$  (see IDF09 and Fragile et al 2007). The LF QPO frequency is then predicted to be

$$\nu_{prec} = \frac{(5 - 2\zeta)}{\pi(1 + 2\zeta)} \frac{a_* [1 - (r_i/r_o)^{1/2+\zeta}]}{r_o^{5/2-\zeta} r_i^{1/2+\zeta} [1 - (r_i/r_o)^{5/2-\zeta}]} \frac{c}{R_g} \quad (1)$$

Simulation data for black holes shows  $\zeta \sim 0$  (e.g. Fragile et al 2007) but neutron stars have a solid surface which could give a rather different situation where the flow is increasingly concentrated on the neutron star surface as the accretion rate increases.

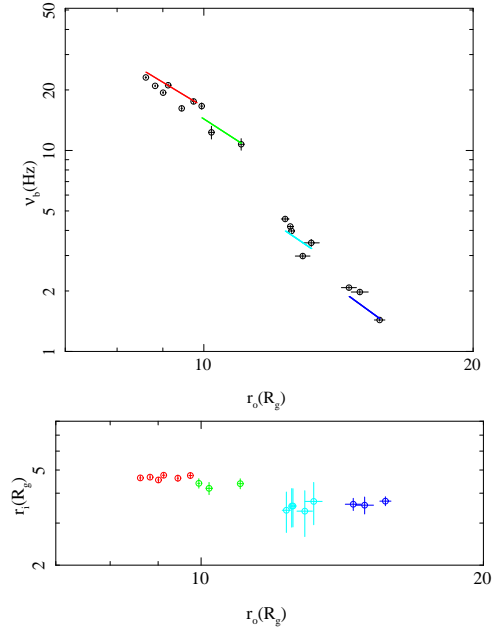


**Figure 3.** *Top panel:* Break frequency plotted against truncation radius,  $r_o$ , with four separate power law fits:  $\gamma = 3.25$  (blue), 3.02 (magenta), 2.88 (green) and 2.69 (red). This treatment assumes that the viscous frequency is given by a power law, the index of which becomes less negative as  $r_o$  reduces.  $\nu_b$  is then  $\nu_{visc}(r_o)$  and  $r_i$  is the value of  $r$  that gives  $\nu_{visc}(r) = \nu_h$ . *Bottom panel:* Inferred values for  $r_i$  plotted against  $r_o$ .

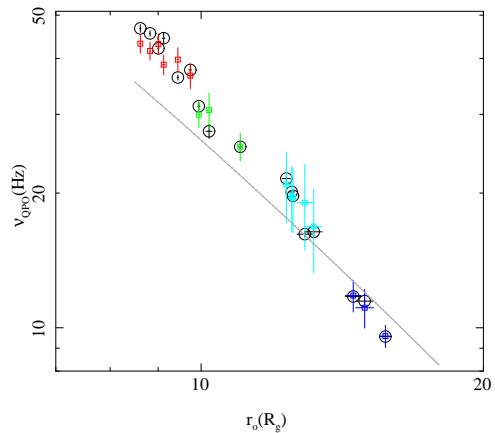


**Figure 4.** LF QPO frequency plotted against truncation radius (black circles). The grey line tracks Lense-Thirring precession frequency of the inner flow with  $r_i = 4.5$  and  $\zeta = 0$ . The blue, magenta, green and red squares are for  $\zeta = -0.7, -0.3, 0.6$  and  $2.7$  respectively and use the  $r_i$  values from the bottom plot of Figure 3.

Nonetheless, assuming  $\zeta = 0$ , and taking  $r_i$  fixed at 4.5 (see previous section) gives quite a good fit (grey line) to the observed LF QPO (black circles) as shown in Fig 4.

The fit can be made even better by allowing  $\zeta$  to vary. As  $r_o$  decreases the expectation is that the flow goes from being similar to the BH case, to being more and more concentrated in the boundary layer i.e. we expect an increase in  $\zeta$  as the dense boundary layer begins to dominate the surface density of the flow. Such an increase in the surface density profile is also implied by the change in viscous frequency implied from the previous section, since surface density

is inversely proportional to the radial velocity  $v_r = R\nu_{\text{visc}}$ . We fit our Lense-Thirring model to the four different sets of points from before and obtain excellent agreement with observation if  $\zeta$  takes the values  $-0.7$  (blue),  $-0.3$  (magenta)  $0.6$  (green) and  $2.7$  (red) i.e.  $\zeta$  increases with decreasing  $r_o$  as expected. However, a quantitative understanding of how these parameters should interact in neutron stars is a very difficult goal as the boundary conditions associated with accreting neutron stars are so poorly understood.

#### 4 CONCLUSIONS

We show that the broadband continuum noise power and LF QPO seen in atolls and BHB can be self-consistently explained in the *same* truncated disc/hot inner flow model which describes their spectral evolution. We test this on the atoll systems, as these have strong kHz QPOs which most probably pick out the truncation radius of the thin disc,  $r_o$ , so this key parameter is known independently. Using the standard assumption that the upper of the two kHz QPOs marks the Keplerian frequency gives that  $r_o$  decreases from  $20 - 8 R_g$  during the marked spectral transition seen in atolls from the hard (island) state to soft (banana branch) spectra.

The low frequency break seen in the noise power is then consistent with being the viscous timescale of the hot flow at  $r_o$ . All smaller radii in the hot flow contribute to the noise power, giving the broad band continuum power spectrum. The highest frequency noise component marks the viscous timescale at the inner edge of the hot flow,  $r_i$ . We use our parameterisation of  $\nu_{\text{visc}}$  to calculate  $r_i$  and find that this remains remarkably constant at  $r_i \sim 4.5 \equiv 9.2 \text{ km}$  for a  $1.4M_\odot$  neutron star.

The truncated disc model also gives a physical interpretation for the observed ‘splitting’ of the lowest frequency noise component seen close to the spectral transition. At this point the spectral models predict that the disc overlaps the hot flow, so there is a component which tracks turbulence in the hot flow *within* the disc inner radius, and another component which tracks the true outer edge of the hot flow which extends over the disc.

With all of the parameters of the truncated disc geometry constrained, we are then able to test the Lense-Thirring precession model for the LF QPO presented in IDF09. This gives a fairly good match to the data at large truncation radii, but increasingly underestimates the QPO frequency as  $r_o$  decreases. Nonetheless, it still only 25 per cent too low even at the smallest  $r_o$ . However, there is still one additional free parameter which is the radial dependence of the surface density of the hot flow. Allowing this to change so that the flow becomes increasingly concentrated towards  $r_i$  as the truncation rate decreases, as expected from the collapse of a hot flow into the boundary layer, gives an excellent match to the data. However, we caution that the expected evolution of the surface density is not well understood quantitatively for neutron stars.

It must also be noted that considering the whole flow to precess removes a previous objection to Lense-Thirring precession as the origin of the LF QPO. If the LF QPO is produced by Lense-Thirring at  $r_o$  then this implies the moment of inertia of the neutron star is too large (Markovic and Lamb 1998). Instead, in our model the LF QPO is produced at some mass weighted radius between  $r_o$  and  $r_i$  with the weight increasingly towards  $r_i$  for softer spectra (higher frequencies). Thus for the lowest values of  $r_o \sim 8.5$ , the LF QPO is predominantly produced by material at  $r_i = 4.5$  rather than at  $r_o$ , so the moment of inertia is correspondingly reduced.

Overall, we present a model of the power spectrum in which both broad band continuum and LF QPO components are inter-

preted physically. This forms a framework in which the characteristic frequencies in the power spectrum can be used as a diagnostic of the properties of the accretion flow in strong gravity.

#### 5 ACKNOWLEDGEMENTS

AI acknowledges the support of an STFC studentship. AI and CD acknowledge useful comments from Chris Fragile, Cole Miller, Didier Barret and the referee Lev Titarchuk.

#### REFERENCES

- Altamirano D., van der Klis M., Méndez M., Jonker P. G., Klein-Wolt M., Lewin W. H. G., 2008a, *ApJ*, 685, 436  
 Altamirano D., van der Klis M., Méndez M., Wijnands R., Markwardt C., Swank J., 2008b, *ApJ*, 687, 488  
 Balbus S. A., Hawley J. F., 1998, *RvMP*, 70, 1  
 Barret D., 2001, *AdSpR*, 28, 307  
 Barret D., Olive J. F., Boirin L., Done C., Skinner G. K., Grindlay J. E., 2000, *ApJ*, 533, 329  
 Barret D., Olive J.-F., Miller M. C., 2005, *AN*, 326, 808  
 Belloni T., Psaltis D., van der Klis M., 2002, *ApJ*, 572, 392  
 Cabanac R. A., Valls-Gabaud D., Lidman C., 2008, *MNRAS*, 386, 2065  
 Chaty S., Haswell C. A., Malzac J., Hynes R. I., Shrader C. R., Cui W., 2003, *MNRAS*, 346, 689  
 Churazov E., Gilfanov M., Revnivtsev M., 2001, *MNRAS*, 321, 759  
 Di Salvo T., Méndez M., van der Klis M., Ford E., Robba N. R., 2001, *ApJ*, 546, 1107  
 Done C., Gierliński M., Kubota A., 2007, *A&ARv*, 15, 1  
 Fragile P. C., Mathews G. J., Wilson J. R., 2001, *ApJ*, 553, 955  
 Fragile P. C., Blaes O. M., Anninos P., Salmonson J. D., 2007, *ApJ*, 668, 417  
 Fragile P. C., Lindner C. C., Anninos P., Salmonson J. D., 2009, *ApJ*, 691, 482  
 Gierliński M., Done C., Page K., 2008, *MNRAS*, 388, 753  
 Gierliński M., Nikolajuk M., Czerny B., 2008, *MNRAS*, 383, 741  
 Ingram A., Done C., Fragile P. C., 2009, *MNRAS*, 397, L101  
 Klein-Wolt M., van der Klis M., 2008, *ApJ*, 675, 1407  
 Krolik J. H., Hawley J. F., 2002, *ApJ*, 573, 754  
 Lyubarskii Y. E., 1997, *MNRAS*, 292, 679  
 Marković D., Lamb F. K., 1998, *ApJ*, 507, 316  
 Medvedev M. V., 2004, *ApJ*, 613, 506  
 Méndez M., 2006, *MNRAS*, 371, 1925  
 Miller M. C., Lamb F. K., Cook G. B., 1998, *ApJ*, 509, 793  
 Misra R., Zdziarski A. A., 2008, *MNRAS*, 387, 915  
 Piro A. L., Bildsten L., 2005, *ApJ*, 629, 438  
 Psaltis D., Belloni T., van der Klis M., 1999, *ApJ*, 520, 262  
 Psaltis D., Norman C., 2000, *astro*, arXiv:astro-ph/0001391  
 Remillard R. A., McClintock J. E., 2006, *AAS*, 38, 903  
 Schnittman J. D., 2005, *ApJ*, 621, 940  
 Stella L., Vietri M., 1998, *ApJ*, 492, L59  
 Strohmayer T. E., Markwardt C. B., Kuulkers E., 2008, *ApJ*, 672, L37  
 Sunyaev R., Revnivtsev M., 2000, *A&A*, 358, 617  
 Titarchuk L., Osherovich V., 1999, *ApJ*, 518, L95  
 Titarchuk L., Osherovich V., 2000, *ApJ*, 537, L39  
 Titarchuk L., Shaposhnikov N., Arefiev V., 2007, *ApJ*, 660, 556  
 van der Klis M., 2005, *Compact Stellar X-Ray Sources*, eds. W.H.G. Lewin and M. van der Klis, Cambridge University Press:astro-ph/0410551  
 van der Klis M., Swank J. H., Zhang W., Jahoda K., Morgan E. H., Lewin W. H. G., Vaughan B., van Paradijs J., 1996, *ApJ*, 469, L1  
 van Straaten S., van der Klis M., di Salvo T., Belloni T., 2002, *ApJ*, 568, 912  
 Wijnands R., van der Klis M., 1999, *ApJ*, 514, 939